

Neutral Hydrogen in the Interacting Magellanic Spirals NGC 4618/4625

Stephanie J. Bush

*Departments of Astronomy and Physics, Case Western Reserve University, 10900 Euclid Ave., Cleveland,
OH 44106*

sjb16@cwru.edu

and

Eric M. Wilcots

Astronomy Department, University of Wisconsin, 475 N. Charter St., Madison, WI 53706

ewilcots@astro.wisc.edu

ABSTRACT

Asymmetry is a common trait in spiral galaxies and is particularly frequent among Magellanic spirals. To explore how morphological and kinematic asymmetry are affected by companion galaxies, we analyze neutral hydrogen observations of the interacting Magellanic spirals NGC 4618 and 4625. The analysis of the H I distribution revealed that about 10% of the total H I mass of NGC 4618 resides in a looping tidal structure that appears to wrap all the way around the galaxy. Through calculations based on derived H I profiles, we show that NGC 4618 and 4625 are no more asymmetric than non-interacting Magellanic spirals analyzed by Wilcots & Prescott (2004). We also derive rotation curves for the approaching and receding sides of each galaxy. By fitting the mean curves with an isothermal halo model, we calculate dynamical masses of $4.7 \times 10^9 M_{\odot}$ and $9.8 \times 10^9 M_{\odot}$ out to 6.7 kpc, for NGC 4618 and 4625 respectively. While the rotation curves had systematically higher velocities on the receding side of each galaxy, the effect was no more pronounced than in studies of non-interacting spirals (Swaters et. al. 1999). The degree of interaction-driven asymmetry in both galaxies is indistinguishable from the intrinsic degree of asymmetry of lopsided galaxies.

Subject headings: galaxies: Magellanic — galaxies: ISM

1. Introduction

Barred Magellanic spirals represent an intermediate phase in the Hubble Sequence between late-type spiral galaxies and irregular galaxies. They are characterized by a single, strong, spiral arm; a bright, off-center bar; and often a high degree of asymmetry in morphology and/or kinematics (de Vaucouleurs & Freeman 1972). While asymmetry is very pronounced in Magellanic spirals, it is also a common characteristic of a large percentage of all disk galaxies (Richter & Sancisi 1994), and therefore important to our understanding of disk galaxies' structure in general.

The frequency of strong asymmetry in spirals has led to a number of different theories to explain its origin. Based on the N-body simulations of Walker, Mihos & Hernquist (1996), Zaritsky & Rix (1997) proposed that minor mergers could induce strong asymmetry in spirals. Their theory is supported by

photographic surveys which found a high incidence of optical companions in Magellanic spirals (Odewahn 1994). However, these models suggest a transient asymmetry, lasting only one or two orbits (Walker, Mihos & Hernquist 1996). Subsequent analytical studies by Sparke and collaborators (Levine & Sparke 1998; Noordermeer, Sparke & Levine 2001) indicate that the one-armed morphology of Magellanic spirals could be quite long-lived if the galaxies’ disks are offset from the dynamical center of the halo. To investigate these theories, Wilcots & Prescott (2004) completed a H I survey of 13 Magellanic spirals from the Odewahn (1994) survey. However, they only confirmed 4 interacting systems. This suggests that current interactions are not responsible for the lopsidedness of Magellanic spirals and that the phenomenon must be longer lived as in the models of Noordermeer, Sparke & Levine (2001). Though the role of interactions in shaping Magellanic spirals is uncertain we cannot escape the observation that many of the prototypical Magellanic (e.g. NGC 4618, the LMC) are part of binary (if not triple) systems. Odewahn (1994) suggested that Magellanic spirals with the highest arm strength also had the most obvious optical companions. However, the effect of binarity on asymmetry is not understood. Here we address whether apparently binary systems are interacting and what effect these interactions may or may not be having on the participating galaxies’ asymmetry and kinematics.

To explore interaction effects and asymmetry, sufficiently detailed studies of galaxies’ kinematics are needed. For example, the model rotation curves presented by Noordermeer, Sparke, & Levine (2001) reflect a disparity between the approaching and receding sides of the galaxy. Additionally, a detailed analysis of the galaxies’ rotation curves allows us to determine the degree to which the halo dominates the dynamics of the galaxy. H I distributions are often more extended than stellar distributions and therefore allow us to derive rotation curves farther into the galactic halo. Extended H I distributions are also better tracers of gravitational interactions. However, sufficiently high resolution H I data only exists for a handful of Magellanic spirals (e.g. Swaters et al. 1999).

We present high resolution neutral hydrogen data for the interacting Magellanic spiral pair NGC 4618/4625. Both galaxies show the optical characteristics of the class mentioned above: a single, strong spiral arm emanating from a bar that appears to be offset from the center of the galaxy (Odewahn 1991). While an earlier H I study of these galaxies did not find evidence of an interaction (van Moorsel 1983), our more sensitive data may. From our data we were able to analyze asymmetry and dynamics by producing H I profiles, velocity fields and rotation curves. These galaxies turn out to be remarkably symmetric, despite their close proximity in the viewing plane. Our observations are explained in §2 and the data is presented in §3. In §4.1 we explore the dynamics of the galaxies, we discuss the nature of the H I loop in §4.2, and we calculate interaction timescales and degrees of morphological asymmetry in §4.3 and §4.4, respectively. We summarize our results in §5.

2. Observations and Data Reduction

Our data was taken using the Very Large Array (VLA)¹ in the C configuration. The integrated time spent on NGC 4618/4625 was ~ 400 minutes in ~ 50 minute sessions, pausing after each session to observe the phase calibrator, 1225+368, for ~ 3 -4 minutes. The amplitude and bandpass calibrator 1328+307 was observed twice for ~ 10 minutes each time. We used the AIPS tasks *vlacalib* and *vlacal* to calibrate the amplitude and phase. The task *imagr* was used to create and CLEAN a naturally weighted image cube.

¹The VLA is part of the National Radio Astronomy Observatory which is operated by Associated Universities Inc., under a cooperative agreement with the National Science Foundation.

Three thousand CLEAN iterations were needed to fully remove the side lobes. Note that a bowl remains in our CLEAN cube. This is the result of the absence of short spacing data and the presence of extended low column density gas. Several line free channels on either end of the data cube were fit and subtracted off the entire cube using the AIPS task *uvlin*. The original cube covered a velocity range of 255.9 km s⁻¹ to 850.4 km s⁻¹, with a velocity resolution of 5.2 km s⁻¹. The final synthesized beam size was 19.6'' × 16.9'' and our final 1σ sensitivity was 2 × 10¹⁸ cm⁻² per channel.

3. Results

Our main results are presented in the moment maps in Figures 1 and 2, which have been smoothed by a factor of 2. These maps also have an applied flux cut of 4σ (8 × 10¹⁸ cm⁻²) in each channel. Along with the integrated H I map, Figure 1 shows H I contours overlaid on an optical image from the Digitized Sky Survey. NGC 4618 is in the southwest at a position of (12^h41^m35^s 41°08'23'') and shows an elongated HI distribution with an H I ring nearly encircling the disk. NGC 4625 is in the northeast at (12^h41^m52^s 41°16'18'') and shows a very large H I disk with a tidal feature extending off the northwest corner. The most striking features of the H I distributions are their large extents and the H I ring encircling NGC 4618. We discuss the nature of this ring in §4.2. We derived radii of the galaxies by calculating the radius of a circle with the area covered by each galaxy. The results were 235.9'' for NGC 4618 and 235.5'' for NGC 4625 down to 3σ (3.54 × 10²⁰ cm⁻²). Adopting effective optical radii of 1.5 kpc and 0.7 kpc, as well as a distance of 6.0 Mpc from Odewahn (1991), we get a ratio of H I extent to effective optical radii of ∼ 4.6 for NGC 4618 and ∼ 9.8 for NGC 4625. NGC 4625 has one of the largest H I/optical ratios of any galaxy yet mapped, comparable to the extent of DDO 154 (Carignan & Purton 1998) and larger than NGC 4449 (Hunter et. al. 1998).

The integrated flux was used to calculate total H I masses of (5.3 ± 0.6) × 10⁸ M_⊙ and (3.9 ± 0.6) × 10⁸ M_⊙ for NGC 4618 and 4625 respectively. Since it was difficult to separate the lower intensity features from the noise at 3σ, these masses were calculated to 4σ (4.72 × 10²⁰ cm⁻²). These are comparable to van Moorsel's H I masses of 4.4 × 10⁸ M_⊙ and 2.8 × 10⁸ M_⊙ (1983). Our slightly increased mass is indicative of our better sensitivity to low column density material such as the H I ring around NGC 4618 and the tidal material extending off NGC 4625 which van Moorsel did not detect. We also calculated the mass in the H I ring on NGC 4618 using 5σ contours to separate the ring from the disk. The east side contains (4.1 ± 0.6) × 10⁷ M_⊙ of H I and the west side contains (5.7 ± 0.6) × 10⁷ M_⊙.

The velocity field is presented in Figure 2. NGC 4625 shows characteristic differential rotation while NGC 4618 has a very disturbed velocity field. We created position-velocity diagrams by rotating the data cube so that the major axis was coincident with one of the principle axes of the cube. These are shown in Figures 3 and 4. Figure 4 shows the P-V diagram for NGC 4625 along the major axis. It is typical of a disk galaxy, with a linear rise in circular velocity at small radii followed by a flat rotation curve. For NGC 4618, P-V diagrams along both the major and minor axes are shown (Figure 3). The diagram along the major axis shows the dynamics of the galaxy disk, exhibiting an almost solid body rotation throughout much of the disk, but with a sharp turnover at large radii that is indicative of the prominent warp evident in the velocity in Figure 2. The P-V diagram along the minor axis gives a clearer impression of the dynamics of the H I ring and will be discussed in §4.2.

4. Analysis and Discussion

4.1. Rotation Curves and Mass Modeling

In order to quantify the dynamics and possible kinematic asymmetry of the galaxies, we fit a tilted ring model to the approaching and receding sides of each galaxies’ observed velocity field (Figure 2) using the AIPS task *gal*. In the models the systemic velocity of the galaxies was held constant at the mean values calculated in §4.4. (The FWZM value for NGC 4618 was not included in the mean used for NGC 4618 because of its strong dependence on the H I ring.) The position of the center of the galaxy was allowed to vary but stayed extremely consistent. The position angle of the major axis and inclination of the disk were allowed to vary and are plotted with the fitted rotation curves in Figures 5 and 6. Note that since the outer portion of NGC 4618 is very perturbed by the interaction, the tilted ring model only fit accurately out to $200''$, 85% of the observed radii. The rotational velocities are consistent with other Magellanic and late type spirals. They are comparable to van Moorsel’s (1983) previous work, with differences of around $10\text{--}20 \text{ km s}^{-1}$ that are most likely due to the van Moorsel’s (1983) constant correction for disk inclination. Van Moorsel (1983) adopted a constant inclination of 35° for NGC 4618 and 27° for NGC 4625, while our fitted inclinations for NGC 4618 range between 40° and 80° and between 20° and 40° for NGC 4625.

It is interesting that both galaxies show an increased maximum velocity on their receding side compared to their approaching side. In NGC 4618, this divergence appears around $100''$, roughly coincident with the edge of the optical disk, and grows as we progress to large radii. The position angle and inclination diverge at about the same point, most likely because at this radii we are analyzing disturbed H I. To the limits of our resolution, NGC 4625 also shows the velocities diverging at the edge of the optical disk. Beyond the optical disk it shows a consistent velocity divergence of about 10 km s^{-1} . The position angle and inclination of either side of NGC 4625 stay roughly consistent with one another, although the position angles show a slow increasing trend. The mean rotation curve of both galaxies flattens at large radii.

To model the dynamical mass we fit an isothermal halo model (De Blok et. al. 2001, Carignan & Purton 1998) to the mean of the approaching and receding sides of the tilted ring models for each galaxy. The isothermal halo has the density profile:

$$\rho_{iso}(R) = \rho_0 \left[1 + \left(\frac{R}{R_C} \right)^2 \right]^{-1} \quad (1)$$

where ρ_0 is the central density of the halo and R_C is the halo core radius. This creates the rotation curve:

$$V(R) = \sqrt{4\pi G \rho_0 R_C^2 \left[1 - \frac{R_C}{R} \arctan \left(\frac{R}{R_C} \right) \right]} \quad (2)$$

The fitted parameters are V_∞ and R_C which relate to the parameters in equations (1) and (2) through:

$$V_\infty = \sqrt{4\pi G \rho_0 R_C^2} \quad (3)$$

We calculate the dynamical mass by numerically integrating equation 2 out to 6.7 kpc. Our fitted parameters were $V_\infty = 65 \pm 15 \text{ km s}^{-1}$ and $R_C = 1.45 \pm 0.33 \text{ kpc}$ for NGC 4618 and $V_\infty = 83.7 \pm 0.4 \text{ km s}^{-1}$ and $R_C = 0.41 \pm 0.03 \text{ kpc}$ for NGC 4625. These values gave central densities of $0.037 \text{ M}_\odot \text{ pc}^{-3}$ and $0.77 \text{ M}_\odot \text{ pc}^{-3}$, respectively. Our fits are shown in Figures 7 and 8. While the fit for NGC 4618 is well within the error bars of the observed rotation curve, the model overestimates the circular velocity of the outer disk of NGC 4625. The mass calculated for NGC 4618 was $4.7 \times 10^9 \text{ M}_\odot$. Adopting B-band stellar luminosities from

Odewahn (1991) and assuming a mass to light ratio of $1 M_{\odot}/L_{\odot}$, we calculate stellar masses of $2.37 \times 10^9 M_{\odot}$ and $0.42 \times 10^9 M_{\odot}$, for NGC 4618 and 4625, respectively. When combined with our calculated H I masses, this gives NGC 4618 a disk mass fraction of 0.6. The fitted mass for NGC 4625 was $9.8 \times 10^9 M_{\odot}$ for a disk mass fraction of 0.08, but since the disk mass to light ratio could be considerably larger than $1 M_{\odot}/L_{\odot}$ this is probably a lower limit. These masses are within the expected range for Magellanic spirals (Wilcots & Prescott 2004) and the disk mass fraction for NGC 4625 is also reasonable. However, the disk mass fraction for NGC 4618 is much higher than we would expect. It has been shown that interactions can strongly affect rotation curves (Barton et. al. 1999) so it is possible that the interaction is affecting the disk in such a way that we see a slowed or truncated rotation curve and calculate a low halo mass.

4.2. Nature of the H I Loop

We explore two different interpretations of the H I ring surrounding NGC 4618. The velocity field and position-velocity diagram of the tidal material surrounding NGC 4618 is indicative of a single tidal arm that fell back towards the galaxy and wrapped around it, forming a coherent loop. The formation of such loops is common in simulations of major mergers (e.g. Hernquist & Spergel 1992, Hibbard & Mihos 1995). The kinematics of the tidal material are apparent in the position velocity diagram of NGC 4618 along its minor axis (Figure 3). NGC 4618’s minor axis is effectively the major axis of the loop. In Figure 3, the tidal material’s dynamics show striking similarity to a solid body rotation curve, supporting the assertion that it is a coherent feature.

Alternately, the loop could be interpreted as a galactic warp possibly created by the interaction, where what appears to be a gap between the galaxy and the ring is actually filled with very low column density gas. If the H I ring is a galactic warp, we can fit a tilted ring model to the H I ring. In order to do this, we spatially smoothed the data cubes by a factor of two, and reanalyzed the data. The derived tilted ring model is Figure 9. The tilted ring model was fit to either side of the galaxy out to $120''$, but was fit better to the entire galaxy beyond $120''$. The rotation curve for the outer portions of the galaxy appears to follow well from the rotation curve from the inner portions, with the exception of three points at radii of 270, 290 and $310''$ that have significantly lower velocities than all other points. Data at these radii lie in the ‘gap’ between the disk and the ring and is not an accurate portrayal of the rotation curve. The apparent continuation of the rotation curve in the outer ring shown would support the interpretation of the ring as a galactic warp. The outer disk has a substantially different position angle than the inner disk, changing from around 180° in the inner disk to around 120° in the outer ring. However it has retained roughly the same inclination, 60° , as the unperturbed disk. This indicates that this structure could be a continuation of the disk, but it does not appear to be a warp in the traditional sense of a change in inclination in the outer portions of the disk (Garcia-Ruiz et. al. 2002). Though it is possible that the H I ring is simply a continuation of the disk, the mass distribution this would imply for NGC 4618 is very unusual, and we believe the tidal loop interpretation is a more coherent picture of the evolution of the galaxy.

However, If the ring is a continuation of the disk, we can use this model to derive a more appropriate mass for NGC 4618. The isothermal halo fit to the data is in Figure 10 (note that the three points in the ‘gap’ were neglected). The derived fitting parameters were $V_{\infty} = 73 \pm 5 \text{ km s}^{-1}$ and $R_C = 1.8 \pm 0.2 \text{ kpc}$, which gave a central density of $0.03 M_{\odot} \text{ pc}^{-3}$, a new mass of $1.1 \times 10^{10} M_{\odot}$ and a disk mass fraction of 0.26. Although this result is more reasonable, it is still significantly larger than the disk mass fraction for NGC 4625.

4.3. Interaction Timescales

Using our observations we can make a few basic arguments about the timescale of the galaxies’ interaction. By dividing the projected distance between the centers of the galaxies (14.5 kpc) by their projected velocity difference roughly de-projected by a factor of $\sqrt{2}$, we calculate the minimum time since the galaxies have interacted to be ~ 0.14 Gyrs. However, this assumes the galaxies are on a completely radial orbit across the line of sight, so the true time to travel even the projected distance is actually several factors larger.

By analyzing the dynamics of H I loop encircling NGC 4618 as a tidal loop, we can estimate the interaction timescale another way. The smooth nature of this loop indicates that the galaxies have only had one close passage, had there been additional close passages we would not expect the shell to survive as a coherent structure (Hernquist & Spergel 1992). By adopting the tidal material’s projected major axis as the radius of its orbit and its velocity at that position as the orbital velocity, we calculate an orbital timescale of ~ 0.5 - 0.7 Gyrs. This is on the same order as each galaxies’ orbital time and significantly larger than the estimate derived above. In addition, it would take the tidal material an additional fraction of an orbit time to leave the disk and enter orbit.

4.4. Asymmetry

The degree of asymmetry for each galaxy can be quantified several ways using H I profiles which are presented in Figure 11. We follow the treatment of Wilcots & Prescott (2004) and measure asymmetry in two ways (Haynes et. al. 1998). First, we calculate the systemic velocity of the galaxies by calculating the full width of the profile at zero intensity, 20% and 50% of the peak. For a completely symmetric galaxy these three values should be equal. Second, we integrated under the approaching and receding sides of the peak and compared the resulting areas. Once again, for a symmetric galaxy they should be equal. The results are in Table 1. Note that, despite its disturbed appearance, NGC 4618’s areal ratio was very close to one, and its FWHM and FW20 are very similar. The FWZM has been strongly affected by asymmetry between the sides of the H I ring and therefore is not a good indicator of the symmetry of the disk. In contrast, NGC 4625 has an areal ratio of 1.3 and a standard deviation of 3.6 km s^{-1} in the systemic velocities.

The striking thing about this symmetry analysis is how morphologically symmetric these galaxies really are, given that they are interacting. We argue above that the interaction between NGC 4618 and 4625 has been ongoing for at least 0.5 Gyr, yet it appears to be significantly affecting only the asymmetry of the outermost gas. In a survey of 13 Magellanic spirals, Wilcots & Prescott (2004) found that the mean areal asymmetry was the same for Magellanic spirals with companions as it was for galaxies without companions (both were 1.1). Similarly, the standard deviation of the median velocities was 9.3 km s^{-1} for galaxies with companions and 7.4 km s^{-1} for galaxies without companions. The H I profile of the *disk* of NGC 4618 is actually *more* symmetric than the average for Magellanic spirals in Wilcots & Prescott (2004).

The interaction is likely to be affecting the galaxies’ kinematic asymmetry as well. Binary galaxies often show asymmetric rotation curves, including examples similar to NGC 4618 and 4625, where one side of the rotation curve falls off while the other continues to rise (Barton et. al. 1999). Each galaxy shows a systematically faster rotation curve on its receding side and it is possible that this is due to disk warping caused by the interaction. However, it is very difficult to determine whether this is truly an interaction effect or if it is an intrinsic trait of the galaxies, as suggested by Swaters et. al. (1999). These authors examined the H I velocity fields of DDO 9 and NGC 4365 and found rotation curves that flattened on one side but continued to rise on the other. However, these galaxies were *not* observably interacting, so their kinematic

asymmetry is most likely intrinsic. From this, we can draw the conclusion that even for galaxies known to be interacting, the possible effects of the interaction, at least in the early stages, are indistinguishable from the intrinsic asymmetry seen in significant numbers of galaxies that are not interacting.

This data reveals that the encounter between NGC 4618 and NGC 4625 appears to be significantly influencing only the outermost H I, which is beyond the optical extent of the galaxy. The impact of the interaction on the inner H I disk, and by extrapolation the stellar disk, appears to be minimal. Yet, both galaxies have strongly asymmetric optical morphologies (Odehahn 1991). The inference one draws is that the current interaction cannot be responsible for the observed degree of asymmetry in the stellar disk, unless the response of the disks to the encounter is incredibly rapid.

5. Conclusions

We have shown that NGC 4618 and NGC 4625 are interacting. The majority of the material exterior to the disks in the system forms a tidal loop encircling NGC 4618 and amounts to $\sim 10\%$ of the total H I mass. One of our most interesting observations is that although the outermost gas on NGC 4618 has been strongly affected by the interaction, NGC 4625 and the inner parts of NGC 4618 seem mostly unperturbed. It is also interesting to note that the velocity fields appear to be unperturbed out to the optical radius of each galaxy, at which point the receding side of the galaxy has a consistently higher velocity. This suggests that the optical component stabilizes the H I disk.

An important factor in explaining the appearance of these galaxies may be the disk to halo mass ratio. We derived total masses of $4.7 \times 10^9 M_\odot$ and $9.8 \times 10^9 M_\odot$ for NGC 4618 and NGC 4625 respectively. When combined with measures of the optical luminosity (Odehahn 1991) and our measures of the total H I mass, we find NGC 4625 has a M_{disk}/M_{halo} ratio of only 8% while NGC 4618's disk accounts for almost 60% of its total mass. Prescott et. al. (2004) use NGC 4618's stellar velocity dispersion to find a disk mass of $2 \times 10^9 M_\odot$, giving a ratio of 40%. Alternately, if the outermost gas on NGC 4618 is interpreted as a warp, we find a total mass of $1.1 \times 10^{10} M_\odot$, giving a disk mass fraction of 26% or 18%. In either case, NGC 4618 appears to have a rather massive disk with respect to the halo. Either NGC 4618 actually does have a particularly low mass to light ratio, or the outer disk or the loss or warping of the outer portions of NGC 4618, have lead to an underestimate of the total dynamical mass.

It is clear that the interaction involves two galaxies with significantly different M_{disk}/M_{halo} ratios. Gerin et. al. (1990) indicate that an encounter between a galaxy with a massive halo and a total mass 1.5 times the mass of the target will result in rapid bar formation in the target galaxy but very slow development in the galaxy with the massive halo. We may be witnessing an interaction that has had the effect of enhancing an already lopsided structure in NGC 4618 while leaving the halo-dominated NGC 4625 relatively unperturbed. The level of disturbance in the morphology of each galaxy's H I distribution may also be explained by how far into the halo the stellar disks extend. Dubinski et. al. (1996) used numerical simulations of merging galaxies to explore how tidal tail strength varies with halo mass and extent and found that galaxies whose halo causes a deeper potential well create weaker tidal tails. If NGC 4625 is embedded in a large extended halo, the halo's deep potential well could have prevented the disk from warping or creating large tidal features.

This work demonstrates the inherent difficulty in understanding the origin of the strong asymmetries characteristic of Magellanic spirals. Our analysis of the asymmetry of NGC 4618 and 4625's H I profiles and velocity fields show no more asymmetry than a sample of non-interacting Magellanic spirals (Wilcots & Prescott 2004). Thus, H I asymmetry is not a reliable indicator of either the presence of a companion

or the effects of an interaction. The asymmetry between the approaching and receding side of the rotation curves are comparable to what Barton et. al. (1999) suggest for binary galaxies as well as to simulations of lopsided galaxies presented by Noordermeer et. al. (2001). Again, this shows how difficult it is to find compelling evidence that the interaction is the cause of the lopsidedness in NGC 4618 and NGC 4625. High resolution observations of other binary systems and a more thorough theoretical examination of the impact of close passages on the structure and kinematics of galaxies with a range of halo strengths may continue to shed light on this problem.

6. Acknowledgments

We would like to thank Dr. Stacy S. McGaugh for allowing us to use his Fortran code to fit dynamical masses and Dr. J. Christopher Mihos for useful discussions about galaxy interactions. This work was supported by a NSF-REU site grant (AST-0139463) to the University of Wisconsin-Madison. EMW was supported by a NSF grant AST-9875008. This research has made use of the NASA/IPAC Extragalactic Database (NED) which is operated by the Jet Propulsion Laboratory, California Institute of Technology, under contract with the National Aeronautics and Space Administration. The Digitized Sky Survey was produced at the Space Telescope Science Institute under U.S. Government grant NAG W-2166. The images of these surveys are based on photographic data obtained using the Oschin Schmidt Telescope on Palomar Mountain and the UK Schmidt Telescope. The plates were processed into the present compressed digital form with the permission of these institutions.

REFERENCES

- Barton, E.J., Bromley, B.C. & Geller, M.J. 1999, ApJ, 511, L25.
- Carignan, C. & Purton, C. 1998, ApJ, 506, 125.
- de Blok, W.J.G., McGaugh, S.S. & Rubin, V.C. 2001, AJ, 122, 2396.
- de Vaucouleurs, G. & Freeman, K.C. 1972, *Vistas in Astronomy*, 14, 163.
- Dubinski, J., Mihos, J.C., & Hernquist, L. 1996, ApJ, 462, 576.
- García-Ruiz, I., Sancisi, R., & Kuijken, K. 2002, A&A, 394, 769.
- Gerin, M., Combes, F., & Athanassoula, E. 1990, A&A, 230, 37.
- Haynes, M.P., Hogg, D.E., Maddalena, R.J., Roberts, M.S., & van Zee, L. 1998, AJ, 115, 62.
- Hernquist, L. & Spergel, D. 1992, ApJ, 399, L117.
- Hibbard, J. E. & Mihos, J. C. 1995, AJ, 110, 140.
- Hunter, D.A., Wilcots, E.M., van Woerden, H., Gallagher, J.S. & Kohle, S. 1998, ApJ, 495, L47.
- Levine, S.E. & Sparke, L. S. 1998, ApJ, 496, L13.
- Noordermeer, E., Sparke, L.S., & Levine, S.E. 2001, MNRAS, 328, 1064.
- Odewahn, S.C. 1991, AJ, 101, 829.
- Odewahn, S.C. 1994, AJ, 107, 1320.
- Prescott, M.K., Wilcots, E.M., Bershadsky, M.A., & Westfall, K. 2004, in preparation.
- Richter, O.-G. & Sancisi, R. 1994, A&A, 290, L9.
- Swaters, R.A., Schoenmakers, R.H.M, Sancisi, R. & van Albada, T.S. 1999, 305, 330.
- van Moorsel, G.A. 1983, A&AS, 54, 19.
- Walker, I.R., Mihos, J.C. & Hernquist, L. 1996, ApJ, 460, 121.
- Wilcots, E.M., & Prescott, M.K.M. 2004, AJ, 127, 1900.
- Zaritsky, D. & Rix, H-W. 1997, ApJ, 477, 118.

Table 1. H I Profile Asymmetries

Galaxy	FWZM km s ⁻¹	FWHM km s ⁻¹	FW20 km s ⁻¹	Mean km s ⁻¹	σ km s ⁻¹	Areal Ratio
NGC 4618	544.7	533.0	534.8	537.5	5.1	1.005
NGC 4625	599.0	605.8	607.4	604.1	3.6	1.29

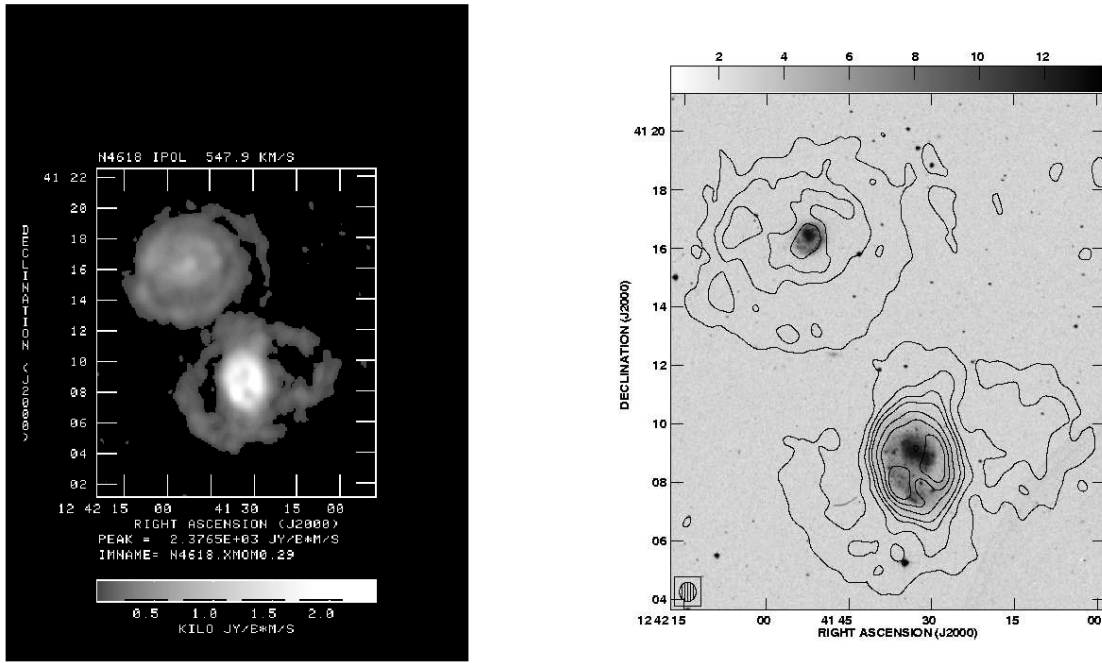


Fig. 1.— The integrated H I map in gray-scale (left) and H I contours overlaid on an optical image from the Digitized Sky Survey (DSS). For clarity, these plots have been smoothed by a factor of 2. H I contours are placed at 5, 10, 15, 20, 30, 40 and 50 $\times (1.18 \times 10^{20} \text{ cm}^{-2})$. The beam is plotted in the lower left corner of the contoured image.

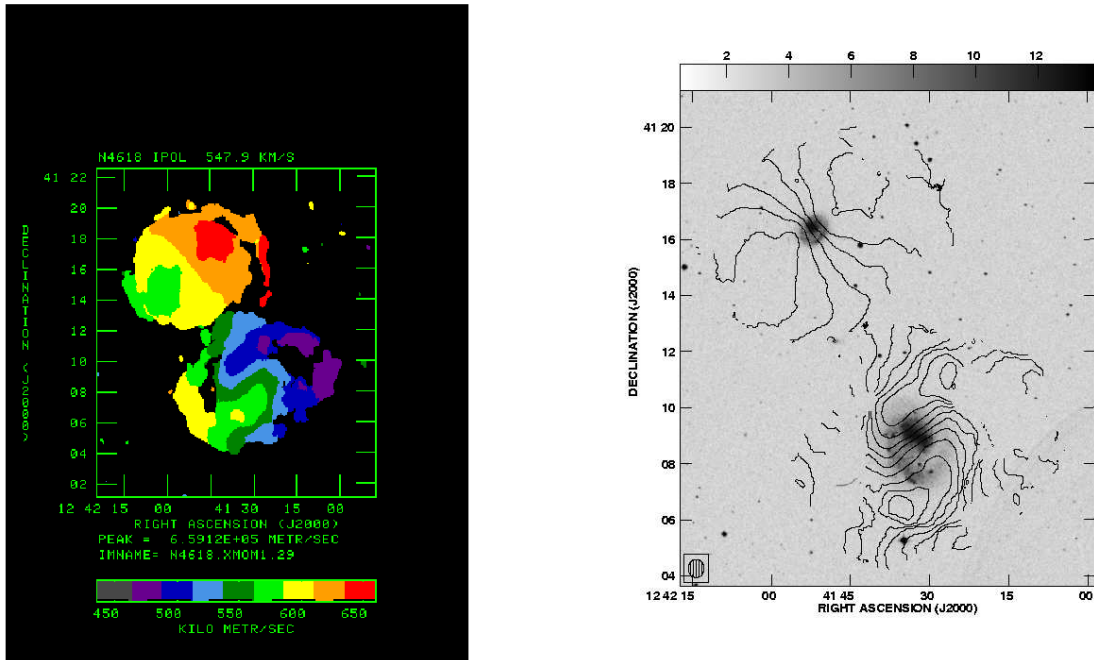


Fig. 2.— The color-coded velocity field (left) and isovelocity contours overlaid on the DSS optical image (right). For clarity, these plots have been smoothed by a factor of 2. Contours are spaced by 10 km s^{-1} . The contours on NGC 4618 increment from 480 km s^{-1} in the northwest to 580 km s^{-1} in the southeast and the contours on NGC 4625 increment from 580 km s^{-1} in the southeast to 630 km s^{-1} in the northwest. Note that the contours on NGC 4618 appear to change abruptly at the edge of the optical disk. The beam is plotted in the lower left corner of the contoured image.

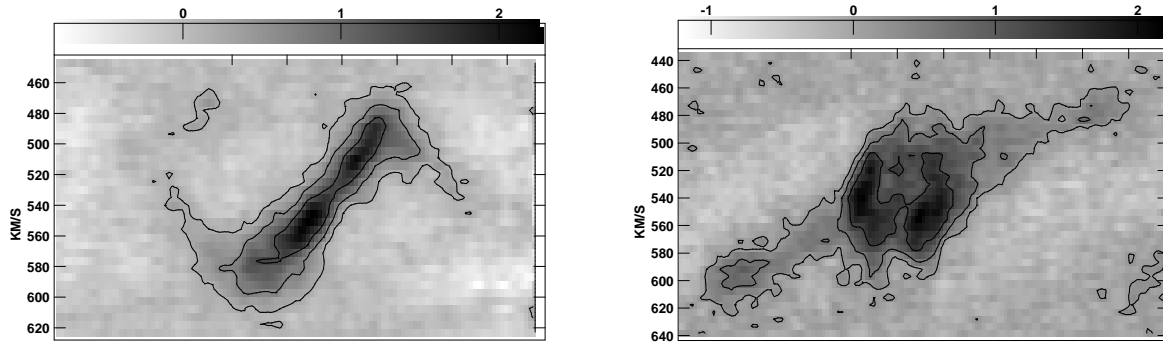


Fig. 3.— Contoured position velocity diagrams for NGC 4618 along the major axis (left) and minor axis (right). The contours are simply used to highlight structure and are at 3, 10 and 20 times the noise in the gray-scale.

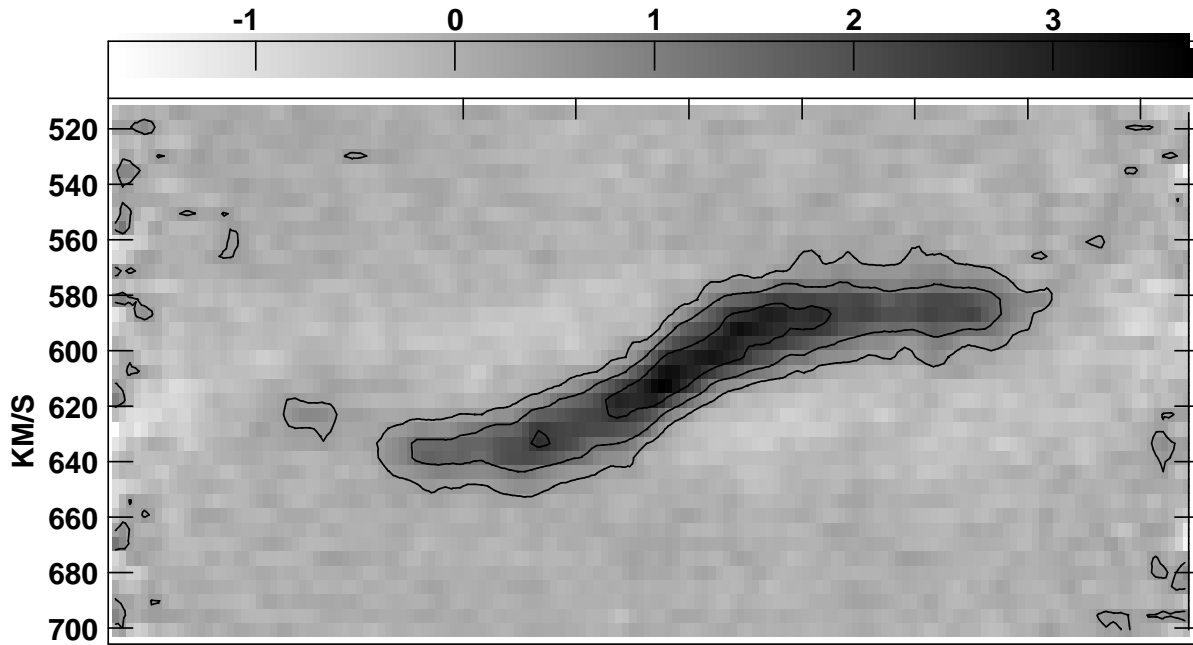


Fig. 4.— Contoured position velocity diagram for 4625. Contours are used simply to highlight structure and are at 3, 10 and 20 times the noise in the gray-scale.

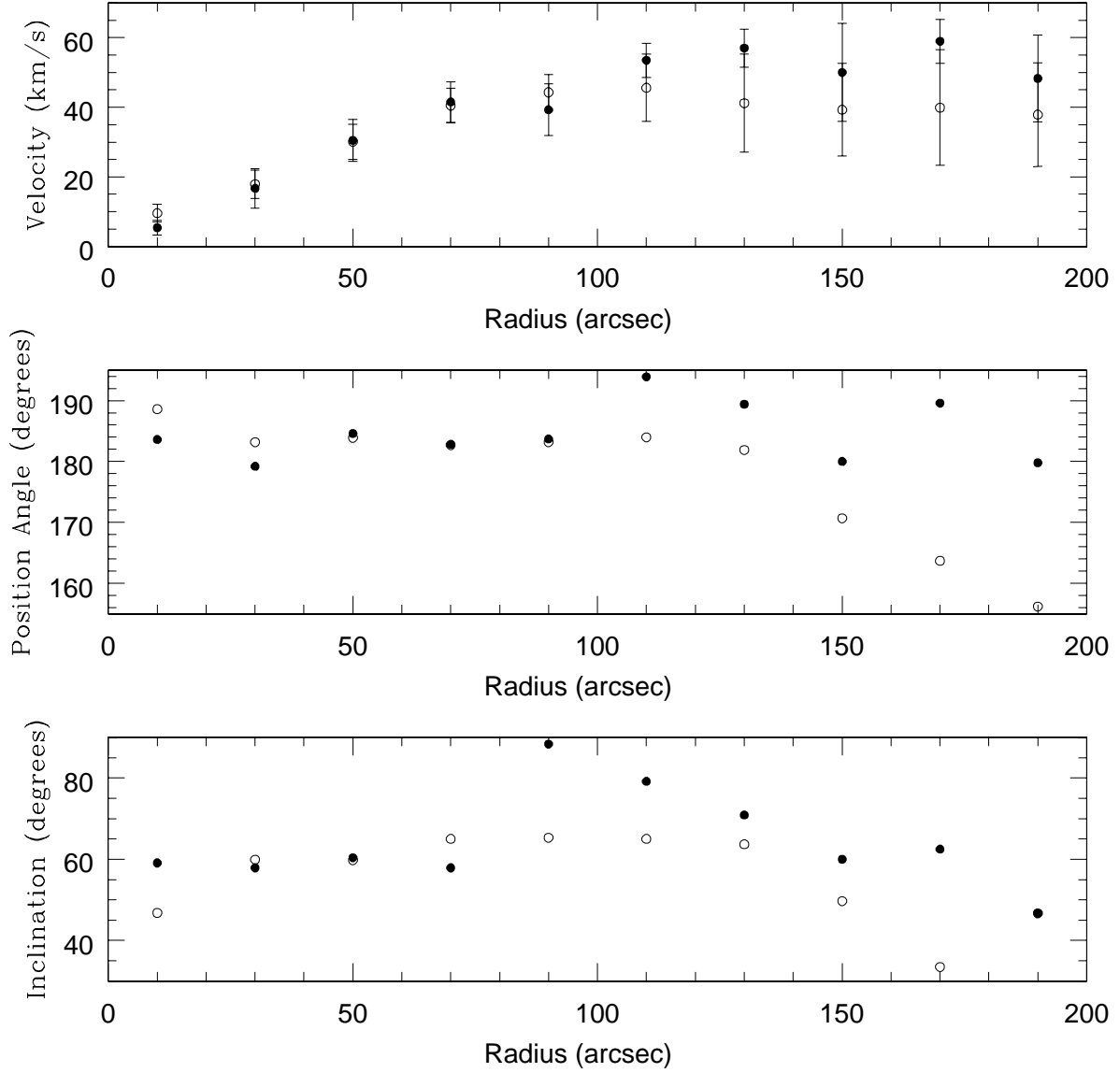


Fig. 5.— Tilted ring model for NGC 4618 with $20''$ rings. Open circles represent the approaching side and closed circles represent the receding side. Error estimates were calculated by AIPS based on the number of points used to fit the model.

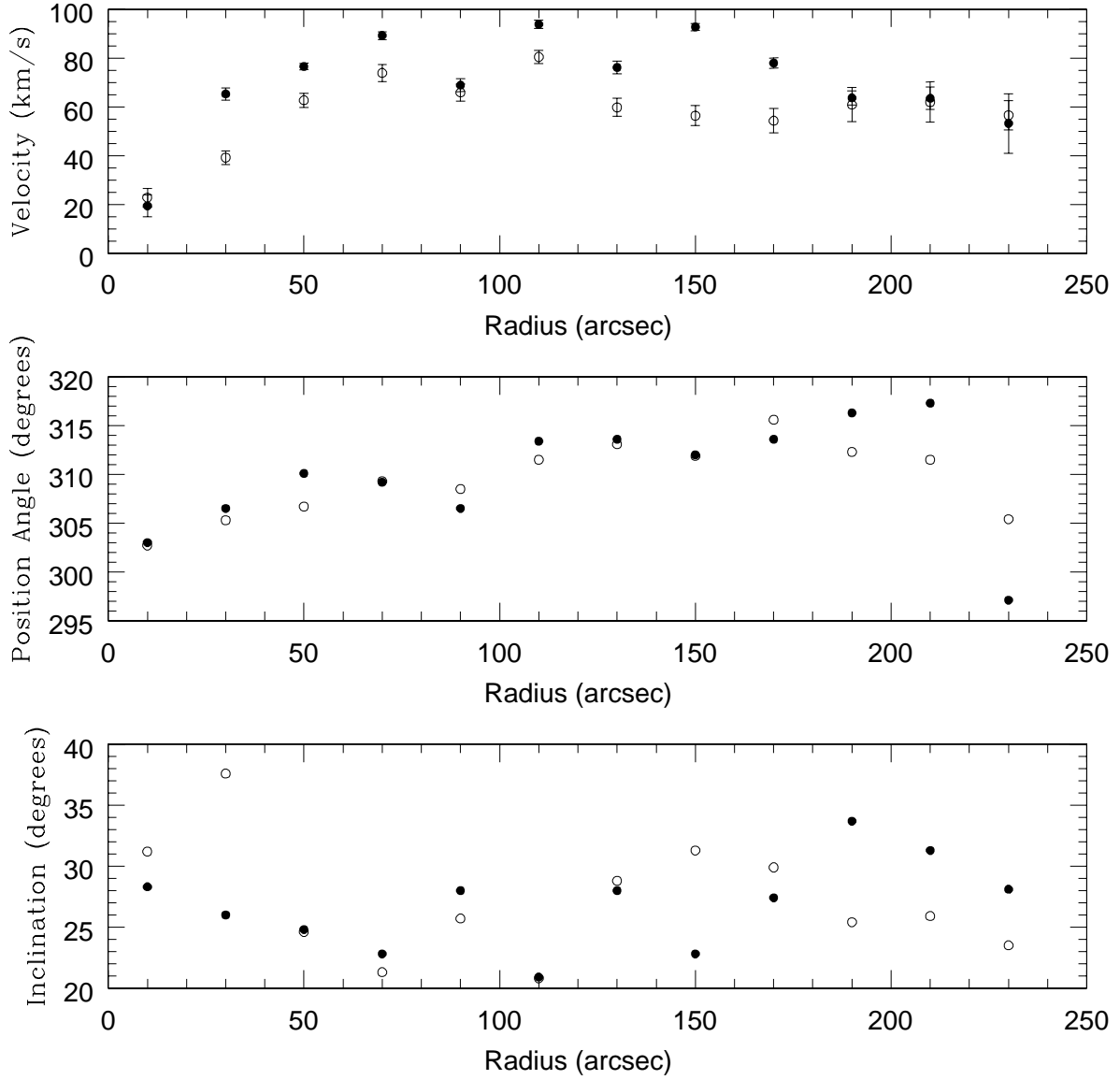


Fig. 6.— Tilted ring model for NGC 4625 with $20''$ rings. Open circles represent the approaching side and closed circles represent the receding side. Error estimates were calculated by AIPS based on the number of points used to fit the model.

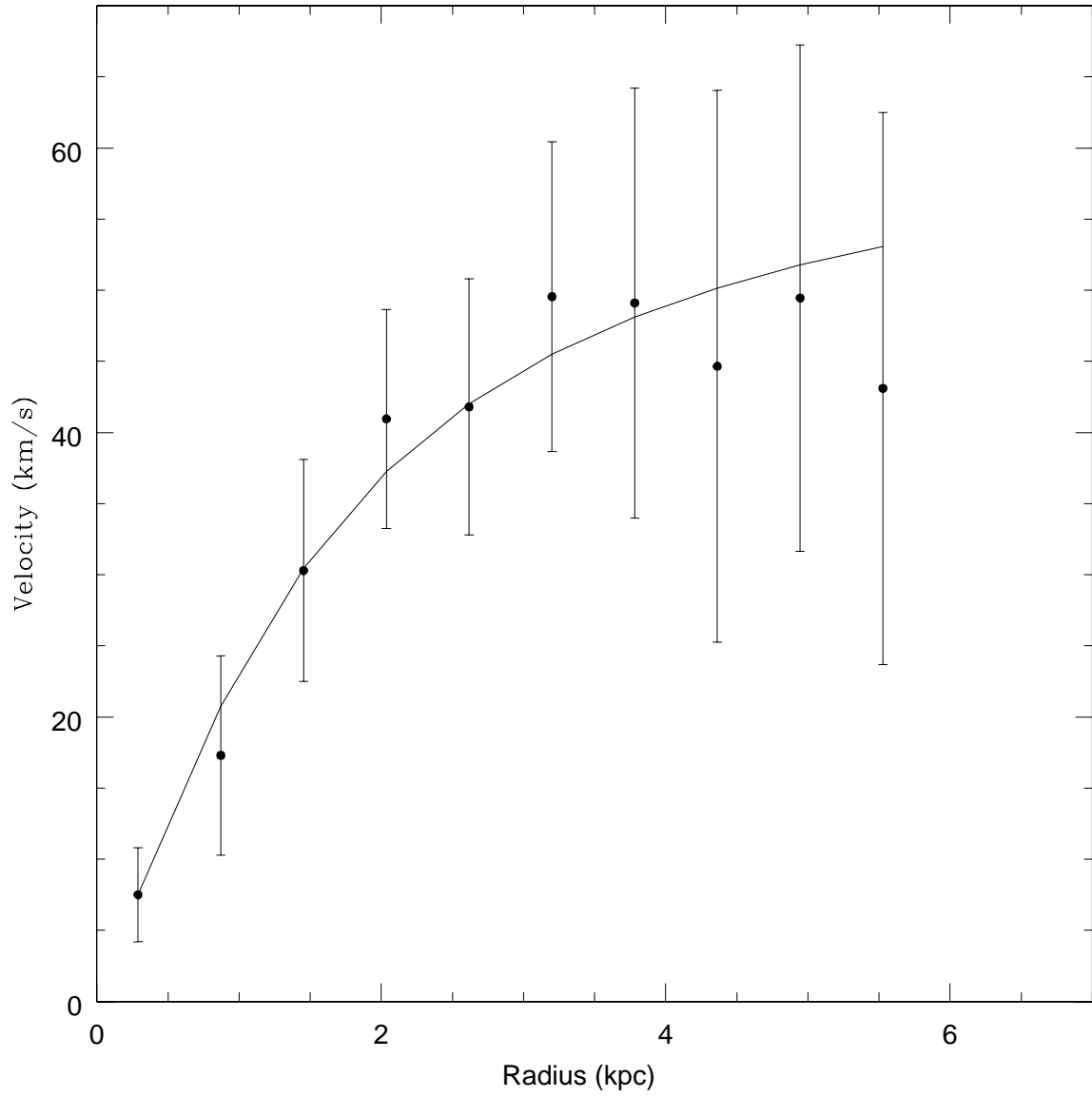


Fig. 7.— Isothermal halo model fit to the tilted ring model for NGC 4618. The radii are computed assuming a distance of 6 Mpc (Odewahn 1991).

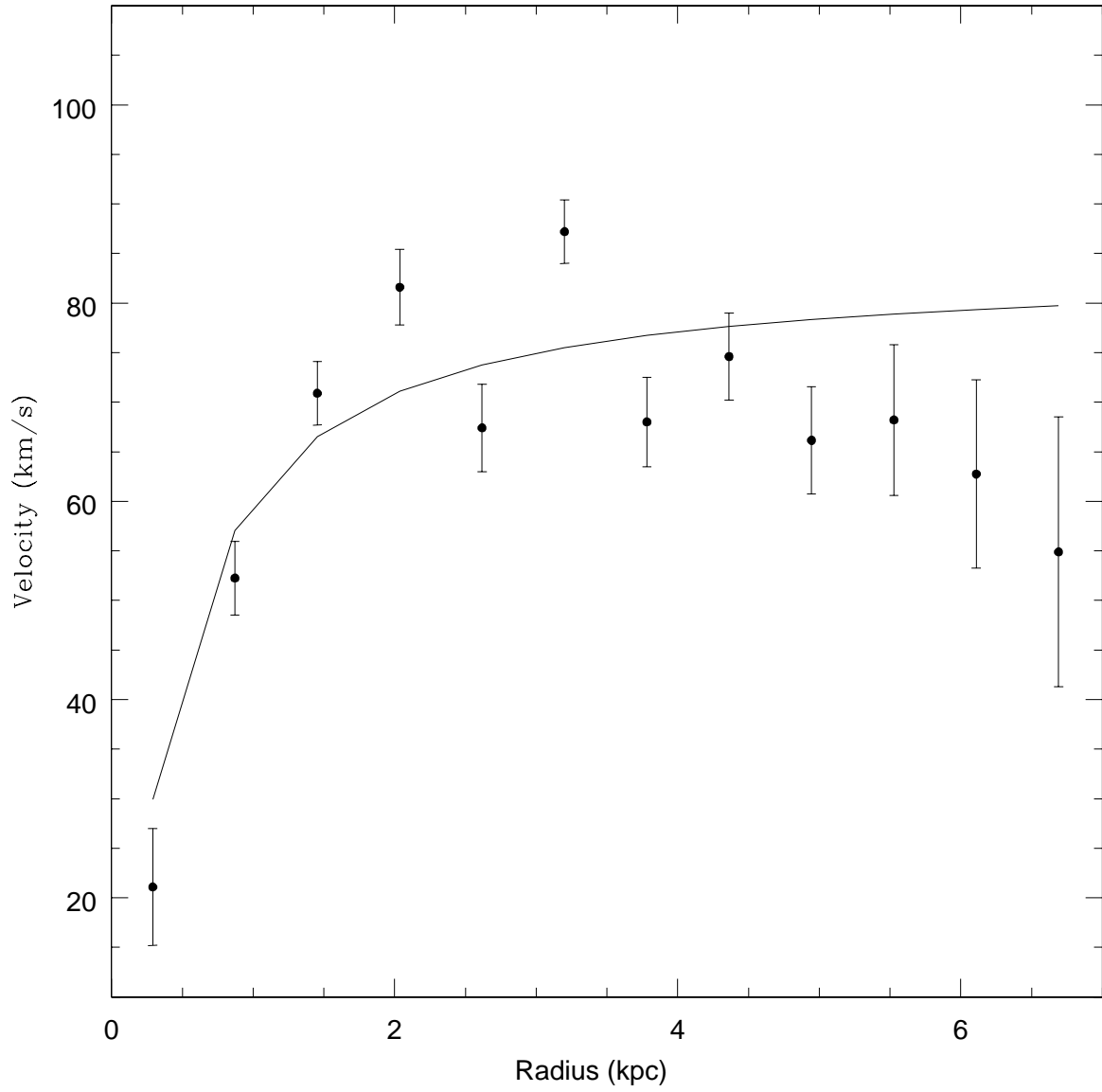


Fig. 8.— Isothermal halo model fit to the tilted ring model for NGC 4625. The radii are computed assuming a distance of 6 Mpc (Odewahn 1991).

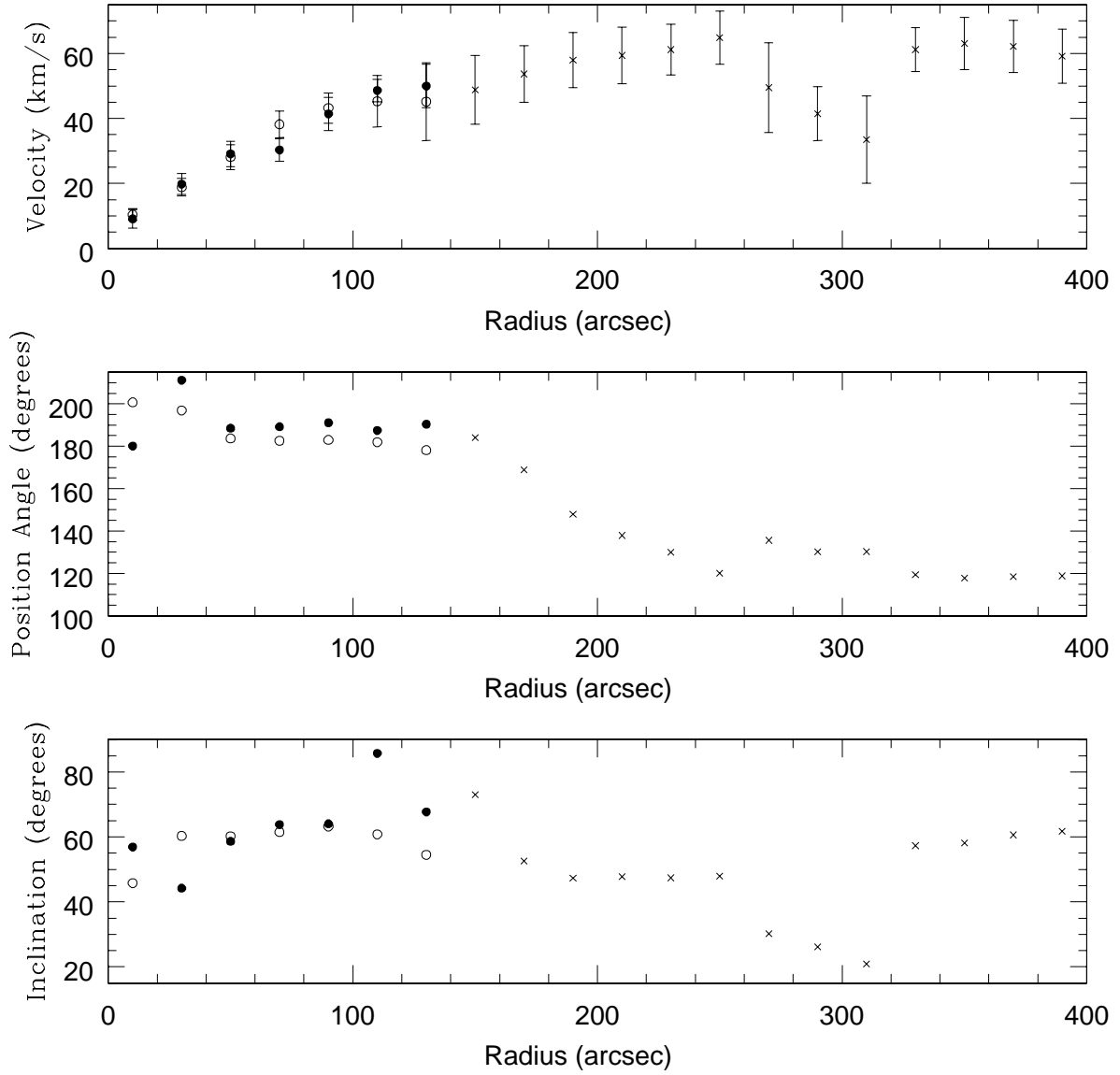


Fig. 9.— Tilted ring model for NGC 4618 with the smoothed data and $20''$ rings. Open circles represent the approaching side and closed circles represent the receding side. Crosses represent the fit in the outer regions. Error estimates were calculated by AIPS based on the number of points used to fit the model.

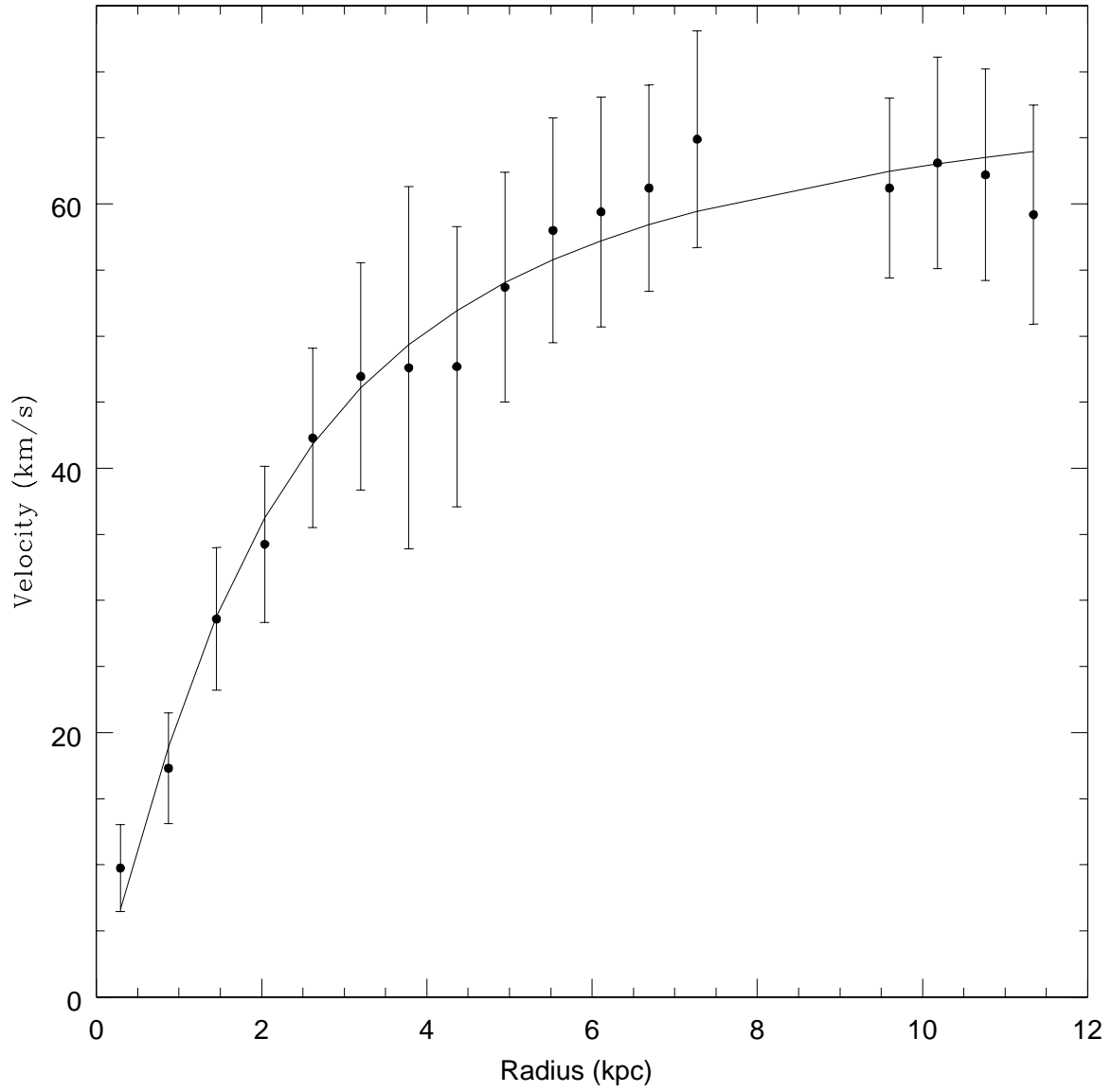


Fig. 10.— Isothermal halo model fit to the tilted ring model for NGC 4618 smoothed data. The radii are computed assuming a distance of 6 Mpc (Odewahn 1991).

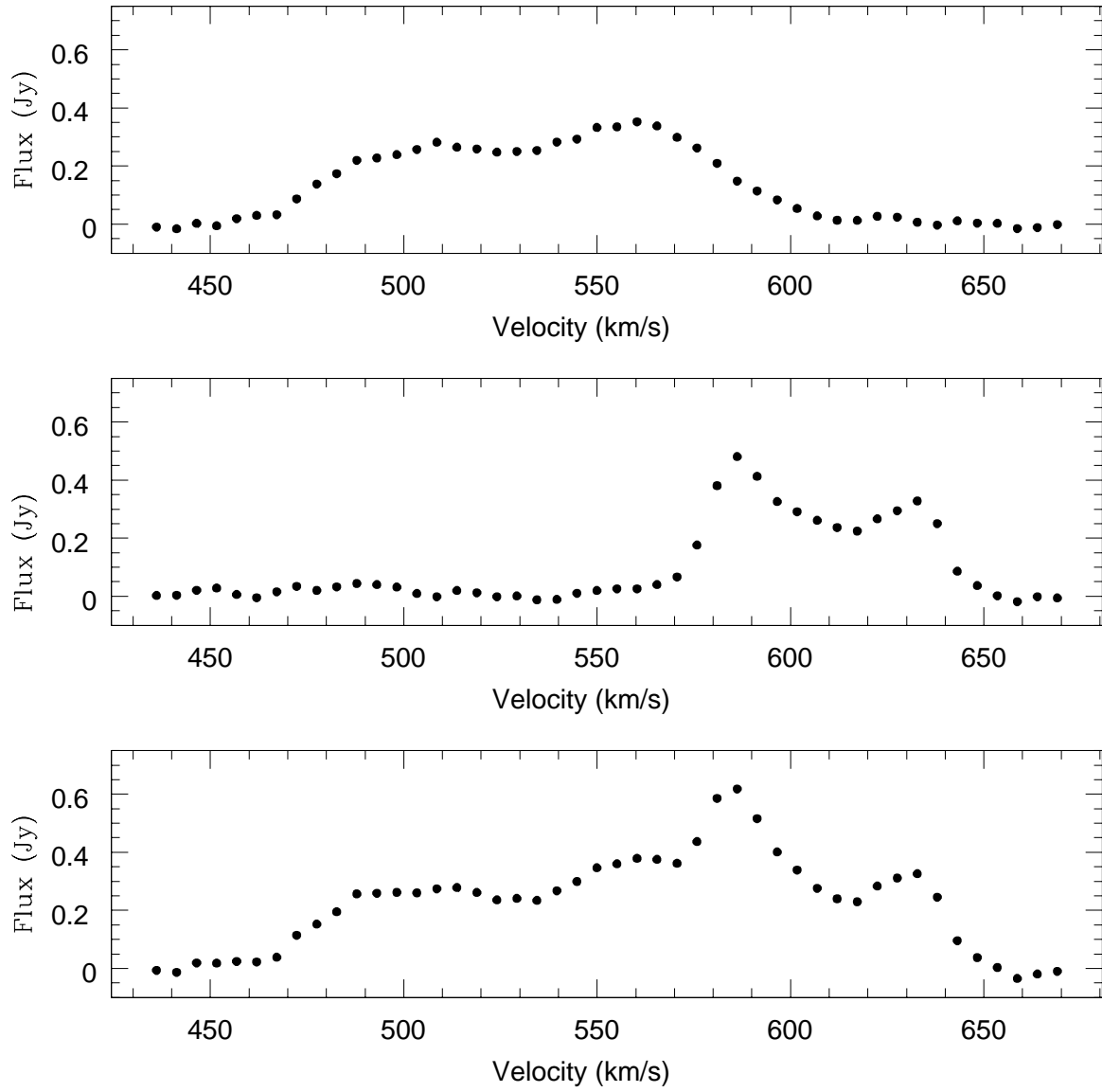


Fig. 11.— H I intensity profiles for NGC 4618 (top), NGC 4625 (middle) and the entire system (bottom).